Energy Conversion and Management 106 (2015) 1295–1308

Contents lists available at ScienceDirect

Energy Conversion and Management

journal homepage: www.elsevier.com/locate/enconman

Process intensification and integration of solar heat generation in the Chinese condiment sector – A case study of a medium sized Beijing based factory

Barbara Sturm [a,b,*], Steven Meyers [c], Yongjie Zhang [d], Richard Law [e], Eric J. Siqueiros Valencia [a], Huashan Bao [a], Yaodong Wang [a], Haisheng Chen [f]

[a] Sir Joseph Swan Centre for Energy Research, Newcastle University, Newcastle upon Tyne, UK
[b] Postharvest Technologies and Processing Group, Department of Agricultural Engineering, University of Kassel, Witzenhausen, Germany
[c] Department of Solar and Plant Technology, University of Kassel, Kassel, Germany
[d] Beijing Association of Sustainable Development, School of Architecture, Tsinghua University, Beijing, China
[e] Process Intensification Group, School of Chemical Engineering and Materials, Newcastle University, Newcastle upon Tyne, UK
[f] Institute for Engineering Thermophysics, Chinese Academy of Science, Beijing, China

ARTICLE INFO

Article history:
Received 3 August 2015
Accepted 15 October 2015
Available online 11 November 2015

Keywords:
SME
Process integration
Solar thermal
PV based hot water and steam generation
Cascading systems
Energetic and economic optimization
Food manufacturing
China

ABSTRACT

Over the last decade, energy prices in China have risen dramatically. At the same time, extensive use of coal fired energy provision systems in industry has led to serious environmental and economic problems translating to an economic damage of an estimated 10% of the Gross Domestic Product. This has led to increasing awareness in the process industries of the need to save energy whilst replacing conventional energy sources with renewable ones.

An energy audit was conducted for a soy sauce production facility in Beijing, which aimed to reduce its thermal energy demand through process intensification and to integrate renewable energy. Their current supply of thermal energy came directly from a district steam network, which was both directly consumed and downgraded via heat exchangers. It was determined that the best two solar integration locations would be in the pre-heating/mixing of raw ingredients to 60 °C and the subsequent direct steaming of the mixture to 120 °C.

Three different systems for supplementing steam were investigated: (1) a traditional solar thermal heating system; (2) a system consisting of mono crystalline photovoltaic panels coupled with either a resistance heater or electric steam generator; and (3) a cascading system consisting of two types of solar thermal collectors, photovoltaic panels, and an electric steam generator. Comparisons of systems 1 and 2 were made for the heating of mixing water, and systems 1, 2, and 3 for saturated steam generation.

Results showed that for the heating of process water, flat plate solar collectors performed best with an estimated 20 year Levelised Cost of Energy of 0.063 €/kW h. Steam generation was most cost effective with a cascade system of photovoltaic and flat plate collectors, with an estimated 20 year Levelised Cost of Energy of 0.145 €/kW h. The model predicts that integration of this technology would lead to a reduction of 14% in heating utility demand.

1. Introduction

In 2011 China was the largest energy user in the world with a total consumption of 12,275 million tons of oil equivalent (21% of the world's energy use). Due to its rapid economic growth, the energy use has increased by more than 150% in the last decade [1], which has increased pressure on energy production. China's industrial sector accounts for almost 50% of the Gross Domestic Product (GDP) and for around 70% of the country's energy use [2]. The industrial sectors contribute more than 82% to the overall national emissions [3].

Coal and oil account for 70% and 18% respectively of the total primary energy consumption. Renewable energy sources currently only deliver 6.7% in total, of which Hydroelectric covers 6% [4]. China's coal consumption, on the other hand, has increased by 200% in the past decade. The extensive use of coal, and in many cases very old technologies in the power plants and boiler houses,

* Corresponding author at: Postharvest Technologies and Processing Group, Department of Agricultural Engineering, University of Kassel, Witzenhausen, Germany.
E-mail address: barbarasturm@daad-alumni.de (B. Sturm).

http://dx.doi.org/10.1016/j.enconman.2015.10.045
0196-8904/

Nomenclature

Abbreviations

CPC	compound parabolic collector
CNY	Chinese Yuan
DHI	diffuse horizontal irradiation
DNI	direct normal irradiation
DR	depreciation rate
EEM	energy efficiency measure
ETC	evacuated tube collector
F&D	Food and Drink
FPC	flat plate collector
FYP	National Economic and Social Development Five Year Plan
GDP	Gross Domestic Product
GHP	gross heat production
IAM	incident angle modifier
IEA	International Energy Agency
LCOE	Levelised Cost of Energy
NPV	Net Present Value
NREL	National Renewable Energy Laboratory
O&M	operation and maintenance
PTC	parabolic trough collector
PV	photovoltaic
SCU	standard coal unit
SD	system degradation rate
SME	small and medium-sized enterprise
ST	solar thermal
UO	unit operation

Symbols

a_1	linear thermal loss coefficient (W/m^2 K)
a_2	quadratic thermal loss coefficient (W/m^2 K^2)
A	area (m^2)
Area	solar system surface area (m^2)
Cost	cost of the solar field
c_p	specific heat capacity (kJ/kg K)
d	day
D	energy demand (kW h/day)
h	hour
H	solar irradiation (kW h/m^2 h)
k	thermal conductivity (kW/m K)
l	length (m)
L	project lifetime (a)
m	mass (kg)
p	peak
$\dot{q}$	heat transmission (kW/m^2)
Q	energy demand (kW h)
$\dot{Q}$	solar energy yield (kW h/h)
r	radius (m)
RCU	relative cost per unit (%)
REC	relative energy consumption per unit (%)
RSS	Ratio Soy Sauce (%)
RV	Ratio Vinegar (%)
s	thickness of layer (m)
S	highest specific solar collector daily yield (kW h/m^2), i.e. "Good Solar Day"
SEC	Specific Total Energy Consumption ($t_{coal,equ}/t_{product}$)
SSD	Specific Steam Demand (t/t)
SWD	specific water demand ($m^3_{water}/m^3_{product}$)
t	time (s)
V	volume (m^3)
W	moisture content (%)
$\bar{Y}$	annual specific collector yield (kW h/m^2 a))
Yield	annual energy yield for solar system (kW h/a)
Δh_e	heat of evaporation (kJ/kg)
α	heat transfer coefficient (W/(m^2 K))
λ	thermal conductivity (W/(m K)
η	efficiency
ϑ	temperature (°C)
ρ	density (kg/m^3)
π	ratio of a circle's circumference and diameter (3.14159)
Δ	difference
θ	solar beam incident angle (°)

Subscripts

1	peak hot water demand
2	peak steam demand
a, amb	ambient
Area	panel area (m^2)
b	bottom
conc	concrete
cond	condensation
dem	demand
e	evaporation
equ	equivalent
ga	gas
gl	glass
h	heating
in	inside
Ins	insulation
l	loss
li	liquid
mix	mixture
O	optical
out	outside
PV	photovoltaic
r	recovery
s	steel
sb	soy bran
so	solid
ss	soy sauce
st	steam
ST	solar thermal
sys	system
t	direct and diffuse irradiation
t	top
tr	transient
v	vat
w	water
wa	waste
wb	wheat bran
wg	wheat grain
wh	waste heat

Superscripts

PV	photovoltaic
ST	solar thermal

has led to serious environmental and economic problems translating to an economic damage of an estimated 10% of the GDP [5]. The Chinese government has addressed this issue through the Renewable Energy Law, passed in February 2005 [6]. The Chinese government has been investing heavily in renewable energy, in an effort to lower China's dependence on coal. With 133 GW of renewable energy technologies installed, China had the largest renewable capacity in the world in 2011.

In 2014, the Chinese national GDP reached a level of 63,600 billion Chinese Yuan (CNY), an increase of 7.4% compared to the previous year. However the increase rate was 0.1% lower than predicted [7]. The GDP increase rate in 31 provinces is generally declining. Guandong province is leading the ranking among all provinces, having generated around 6780 billion Yuan in 2014, followed by Jiansu province contributing 6510 billion Yuan to the overall GDP. 8 provinces or municipalities have joined the 'per capita GDP 10,000 US dollars' Club: Beijin, Tianjin, Shanghai, Zhejian, Jiansu, Inner Mongolia, with Guandong and Fujian joining in 2014. Beijing's GDP reached 2133 billion Yuan, an increase of 7.3% compared with the previous year. Beijing is the most representative city in experiencing rapid urbanization and economic growth, accelerated changes in technology, as well as increasing energy consumption and carbon emissions. In 2010, the total energy consumption reached 69.54 Mt_{ce} and, correspondingly, the per capita energy consumption was at a level of 3.54 t_{ce}, 1.5 times the national average, ranking only second to Shanghai [8]. The per capita CO_2 emissions reached 6.91 tonnes in 2009, i.e., 1.3 times the national average [9]. Beijing is also characterized by a scarcity of natural resources, indicated by the fact that all the natural gas and crude oil consumed by the city, as well as 95% of the coal, 64% of the electricity, and 60% of the refined oil consumed, has to be imported [10].

Within the 11th and 12th National Economic and Social Development Five Year Plan (FYP) the central government introduced a number of measures to increase energy efficiency and environmental performance of the producing industries. The 11th FYP targeted a reduction of specific energy intensity of products by 20% by the year 2010 and the 12th FYP aimed for a reduction of 40–45% by 2020 compared to 2005 levels [11]. The 2010 target was only narrowly missed with an overall reduction of 19.1% [12]. The most representative central policies introduced within the 11th FYP were the Top-1000 Enterprise Program, Ten Key Energy-Saving Projects and the Obsolete Capacity Retirement Program. Responsibility for the measures lies with the sub-national governments. Several provincial and municipal governments have introduced their own programs. In 2006, Shangdong Province initiated a key enterprise program which by 2012 had led to 70% of all provincial energy consumption being covered by energy saving responsibility contracts. In 2007, Shanxi Province initiated the "Double 100 Program" which by 2008 had been extended to 996 companies [13]. In 2011, the Municipal Government of Beijing released a list of recommended energy audit consulting entities [14] to formalise the procedures and secure the quality of energy audits. Shen et al. [11] gave a comprehensive overview of industrial energy audits in China. With the introduction of the Cleaner Production Promotion Law, which has a set of mandatory aspects, China became the first country in the world to make cleaner production at least partially mandatory. Bai et al. [15] gave a comprehensive overview of the measures on central and provincial government level leading to this law. Industrial energy audits have become a key aspect of China's efforts to reduce its energy intensity and overall rise in energy demand.

Whilst energy efficiency has been recognised as an important means to increase the competitiveness of companies, the sole focus in the past was on large and very energy intensive companies. However, in most industries, small and medium sized companies (SMEs) are far more energy intensive due to economy of scale and other barriers which were extensively discussed by Thollander et al. [16] and Trianni et al. [17]. Only recently have SMEs been specifically targeted by including them into policies, measures and dedicated funding mechanisms [16]. Particularly in SMEs of the Food & Drink (F&D) sector energy costs usually only marginally contribute to the overall production costs (<5%) and therefore only get limited attention from a financial perspective [18]. Furthermore, there is a great fear of negatively impacting the product quality by modifications of the systems and often only very limited knowledge regarding energy efficiency is present in the companies [19]. Increasing energy and raw material costs as have been seen over the last decade have been threatening the livelihoods of many food manufacturers [20]. It needs to be noted, that the increased raw material prices often almost marginalised the increase of energy prices which further reduces the focus on these. Thus, to date energy efficiency measures (EEM) have rarely been applied. In a case study conducted by Primabodo and Kumar [21], the authors found the small companies in the F&B sector to be the most energy intensive (energy consumption per value added) of all compared sectors.

For the above reasons producing companies are under growing financial and legislative pressure. Therefore, these companies are increasingly looking for opportunities to replace conventional energy sources with other, more cost effective and sustainable alternatives.

Two-thirds of all industrial energy demand is used for process heat, 13% at temperature levels below 100 °C and 27% below 200 °C [22]. Thus, there is a huge potential for the integration of solar PV and thermal energy in the processing industry, particularly in China. However, at present, the annual global production of solar process heat only covers ca. 0.5% of the global demand [23]. The main areas of application are the food, textile and chemical industries, as well as general cooling and air conditioning applications. The International Energy Agency IEA [24] predicted the solar process heat capacity of China's industry to be 179 GW_{th} in 2020, 435 GW_{th} in 2030 and 1125 GW_{th} in 2050. The IEA also estimated that, given policy making for adopting PV, installations could grow from 18 GW installed in 2013, to 634 GW in 2030 and 1738 GW in 2050, potentially capturing nearly 40% of the global installed capacity [25].

1.1. Process integration and integration considerations for solar process heat

In many industries the allocation of energy to processes is known at a financial level at best [26]. Therefore, it is often necessary to carry out production and energy audits. The calculations of thermal energy demands are usually carried out on a unit operation (UO) level, based on production data and manufacturer information on technologies used. This allows for the generation of a detailed energy and mass balance in each component. The data gathered is also compared to bench marks within the industry for evaluation of their own performance. It is imperative to also calculate the theoretical thermal energy demand for the key processes to be able to evaluate the respective efficiencies and evaluate whether replacement of technology or improvement of insulation would be useful.

Schmitt [27] developed a methodology to assess the feasibility of the integration of solar thermal systems in the processing industry. This methodology can generally be divided into three main parts and consists of nine steps in total: pre-feasibility assessment (basic data acquisition; preparation), feasibility study (company visit; analysis of status quo; process optimisation and energy efficiency; identification of integration points; analysis of integration points) and discussion/further steps (decision; detailed planning).

Generally, two different approaches can be distinguished: integration on the supply level and integration on the UO level. Also, in integration of renewable energy sources, it is very important to first always evaluate the potential for process integration. The IEA SHC TASK 49/IV Integration Guideline [28] gives a good understanding of the options available. Only when the process is optimised, will integration of solar thermal technologies show the real benefit. One of the great challenges in the food industry

is that many processes are operated in batch mode. Furthermore, with solar energy being intermittent, heat storage becomes a necessity [28].

1.2. Solar heat generation

The type and design of the solar thermal system used depends on 4 factors:

1. The diurnal changes in ambient temperature.
2. The seasonal change in ambient temperature and solar radiation.
3. The ratio between direct and diffuse radiation.
4. The water or steam temperature required.

The minimum efficiency of the system is determined by the water/steam temperature required in winter. There are two main types of solar thermal systems to be differentiated: (a) passive, which use convection or heat pipes to circulate the hot water; and (b) active systems, which use a pump. Three types of collectors are commonly used: flat plate (FPC, 30…80 °C), evacuated tube (ETC, 50…200 °C), and concentrating (CPC (60…240 °C) or PTC (60…300 °C)) collectors [23]. Although varying in design, their main purpose stays the same: converting solar radiation into heat to satisfy the thermal energy demands. The harnessed energy can either be used directly or stored for later use. The collector efficiency depends significantly on the type of collector chosen and its operating temperature. Besides the stationary solutions there are single-axis tracking and two-axis tracking systems available. These systems have a higher efficiency at higher temperatures due to the reduction of convective and radiative losses stemming from a smaller absorber area. Muster et al. [28] give an overview of different types of collectors which are commercially used.

Although there is a great need for low grade heat in the food industry, and is therefore an ideal application for solar thermal energy, hardly any applications exist [26,28]. Integration of solar thermal systems into existing processes cannot be generalised and has to be evaluated anew with every specific case as the market is extremely fragmented.

PV systems classically are used to produce electricity which is then directly consumed or transmitted to the public grid. Conversion efficiencies are much lower than those of solar thermal systems, up to 75% less. The design and installation of solar PV systems are significantly simpler. As opposed to solar thermal systems, there are no moving parts (i.e. pumps and fluid), and the problematic of discharging the heat in times of no demand does not exist, as electricity can always be consumed by other users, supplied to the grid or stored in batteries.

1.3. Optimum solar system design, including energetic and economic aspects

Weinstock and Appelbaum [29,30] define optimum solar field design as a constrained optimisation problem considering aspects such as optimum row distance and therefore reduction of shading, maximum energy output, minimum plant cost and minimum cost per unit energy. For this purpose they present algorithms for the optimisation of single stage stationary systems.

As described in Section 1.2, every solar thermal collector has an optimum temperature band in which its efficiency is the highest. Collectors for low temperatures are the cheapest but also require the most space. Commonly, if a higher temperature is required, collectors are chosen which can produce these temperatures. However, the cost efficiency of the overall system relative to the low temperature collectors is significantly decreased while operating in lower temperature regions, where cheaper systems should be used with higher efficiencies. Production of process heat utilising solar PV and a resistance heater is showing signs of becoming more cost effective at higher temperatures, particularly in regions with a high proportion of diffuse irradiation. Consequently, for systems with high differences between incoming and outgoing temperature of the working medium, a cascading system consisting of different types of solar thermal collectors and solar PV for the final boost is a promising alternative for these systems. To date, there are no such systems implemented in industry and only little research on this topic is available.

1.4. Soy sauce production

Soy sauce is becoming increasingly popular on the global market. In 2006, 7.5 Mio m^3 of soy sauce were produced globally with an estimated increase of production to 8.3 Mm^3 by 2020 [31]. There are two main methods for the production of soy sauce, fermentation and acid hydrolysis. The market shares of the two are estimated to be almost equal. The production process for traditionally produced soy sauce consists of three major steps, Koji production, brine fermentation and refining as described by Luh et al. [32]. In contrast, in acid hydrolysis the raw materials are hydrolysed, neutralised, refined, treated with active carbon and filtered [33]. The latter product is significantly different to the former regarding its composition. Technologically the processes also differ greatly. This has direct implications on the degree of mechanisation and process integration possible, the production time (hydrolysis <24 h, semi traditional and traditional 25–70 d), and the average energy demand per unit produced.

Based on a case study in the greater Beijing area, the work presented investigates energy demand patterns, the potentials of process integration through retrofitting, and the substitution of parts of the energy demand by integration of solar process heat. An energetic and economic solar field optimisation analysis is presented for three to generate solar process heat: (1) single stage solar thermal, (2) single stage solar PV with electric hot water and steam generation and (3) a cascading solar thermal and PV combined system.

2. Case description: The production facility for soy sauce

The site investigated is a medium-sized soy sauce plant in the greater Beijing area, co-located with a vinegar plant. The factory is part of an industrial park which is centrally supplied with process heat in the form of steam by a steam plant. The owner company also owns a number of other food and food condiment plants in several other provinces. The site in Beijing produces soy sauce and vinegar, both in a semi-traditional way. The vinegar plant was completely replaced in May 2009, leading to significant reductions in specific overall energy demands. However, according to the production manager, the change of system led to substantial changes in the taste of the product and, consequently, a reduction in the market share. Although the vinegar plant is not part of the core case study, the information on energy demands is only available on a site level and, therefore, the demands for vinegar production have to be considered. Further, the fact that a significant part of the market share was lost due to changes in the taste, shows how crucial it is to not interfere with the production process unless the correlation between product quality and processing is known in detail.

2.1. The energy supply on site

On site, the energy sources used are steam, electricity, natural gas and petrol. Heat has by far the highest share in the energy mix at almost 90% and is supplied by the central steam plant.

The steam supply temperature is at 152 °C (0.37 MPa) and the system is open.

The data related to energy use was only available on a total site level, which includes the soy sauce production line as well as the vinegar production line, with no possibility to reliably split between the two. Petrol is almost exclusively used for running the vehicle, whilst natural gas is used as backup for the steam supply which, regarding the low share at less than 1%, occurs very rarely. All energy sources were converted into standard coal units (SCU) using the standard conversion factors.

2.2. Soy sauce process description

The daily production capacity is 8 batches in 10 h. Fig. 1 shows a process flow diagram of the process investigated. The ratio of raw materials is soy beans/wheat/wheat bran 50:20:30%. In the first production step, the soy bean and the wheat flakes are mixed and then water is added at 90 °C. The resulting mix is then stirred for 30 min after which the wheat bran is added. Then the mix is steamed for another 30 min and heated to 120 °C using direct steam injection. After steaming, the mix is emptied on a conveyor belt where it is cooled to 40 °C using forced air cooling. On a second conveyor, belt the yeast is added to the mix. The pre-fermentation is carried out in flat, long vats (20 in total, 10 for each fermentation line) that are open to the atmosphere. The vats are grouped in twos in separate rooms where the temperature is controlled manually using wall mounted radiators. Two vats accommodate 3 batches produced. The mix stays in pre-fermentation for 24 h and is then transferred to the fermentation vats via a conveyor belt.

The fermentation vats are grouped in two halls in units of 40, 4 of which share one water bath. Each vat accommodates 2 production batches. Fermentation is performed for 26–27 days at 50 °C and the vats are open to the atmosphere on the top side. In the vats, salty water is added to the mix. The bottoms of the vats consist of a perforated metal plate, which is permeable for the liquid but not for the solids. The liquid is collected underneath the plate. For the first 10 days the mix is not disturbed, after that the accumulated liquid is recirculated on the upper surface of the mix for 40 min every day. This recirculation is conducted to increase the degree of extraction from the mix. After 27 days the soy sauce is drained, sterilised, cooled and bulk stored. The fermentation residue is then manually removed and consequently used as animal feed.

The water baths are heated through direct steam injection, the overflow water is discarded of at 55 °C. There is no control system implemented. Every water bath has a manual temperature gauge installed which is regularly checked in a walk through assessment. As soon as the temperature of the water bath falls below 55 °C, the shop floor workers will open the steam valve until the displayed water bath temperature has risen to 60 °C.

The production halls are heated using a central heating system with standard radiators. The supply temperature of the system is 95 °C and the return temperature is 70 °C. The water is heated in a storage tank through a steam-water heat exchanger, the condensate is discarded of at a temperature of 98 °C. The soy sauce is sterilised at 115 °C using 152 °C steam and exits the unit at 110 °C. The incorporated heat is recovered and used for pre-heating the water which for producing the salty water, and is stored at 50 °C in two insulated storage tanks.

3. Methodology

3.1. System and energy audit

In the present case the operations involved are: mixing and cooking of the raw materials, pre-fermentation, fermentation, sterilisation and space heating, see Fig. 1. Much like in other companies in the F&D sector [19], the data acquired by the company by default was not sufficient for the conduction of a detailed energy audit. Therefore, detailed measurements were necessary and assumptions for values which could not be measured had to be made based on experience of the auditors and literature data. Energy and production data of 5 consecutive years were available for the total site. This included vinegar and soy sauce production data, which were available split by the month. All values in this section are based on the theoretical demand and losses.

3.1.1. Steam supply and condensate losses

Steam supply calculations were based on the theoretical energy demand of each production step. It was assumed that there were no losses in the heat transfer and that the condensate left the steam heat exchanger at a temperature of 98 °C and was discarded. Steam supply temperature was assumed at 152 °C, which is contractually guaranteed at the hand over point from the steam network. All potential losses on site due to leakages or inferior insulation were not regarded. The mass of steam used was directly based on the sum of all theoretical energy demands and heat losses in the stage in question, which are described in detail below. Steam demand was calculated as follows:

$$m_{st} = \frac{Q_{dem}}{(\Delta h_e + c_{p,st} \cdot \Delta\vartheta)} \quad (1)$$

For the heat loss calculations related to the discarded condensate, a baseline temperature of 20 °C was used. Calculations were conducted as follows:

$$Q_{cond} = m_w \cdot c_{p,w} \cdot \Delta\vartheta \quad (2)$$

3.1.2. Cooking and steaming stage

The physical and thermodynamic properties of the raw materials were used as follows [34,35]: soy bean bran $c_{p,sb}$ = 1.85 kJ/(kg ∗ K), k_{sb} = 0.034 W/(m ∗ K), W_{sb} = 6.1%, ρ_{sb} = 620 kg/m^3, m_{sc} = 1250 kg; wheat $c_{p,wg}$ = 1.46 kJ/(kg ∗ K), k_{wg} = 0.06 W/(m ∗ K), W_{wg} = 8.0%, ρ_{wg} = 324 kg/m^3, m_{wg} = 500 kg; wheat bran $c_{p,wb}$ = 1.46 kJ/(kg ∗ K); k_{wb} = 0.051 W/(m ∗ K), W_{wb} = 8.0%, ρ_{wb} = 171 kg/m^3; water $c_{p,w}$ = 4.2 kJ/(kg ∗ K), ρ_w = 1000 kg/m^3, $\Delta h_{e,w}$ = 2258 kJ/kg m_w = 1750 kg; values for the mix: $c_{p,m}$ = 2.8 kJ/(kg ∗ K), ρ_m = 685 kg/m^3, Soy sauce: $c_{p,ss}$ = 3.8 kJ/(kg ∗ K), ρ_{ss} = 980 kg/m^3.

The energy demand for heating of the raw materials was calculated using Eq. (3)

$$Q_h = (m_w c_{p,w} + m_{sb} c_{p,sb} + m_{wg} c_{p,wg} + m_{wb} c_{p,wb}) \cdot \Delta\vartheta \quad (3)$$

For estimation of losses in the cooking and steaming stage, the cooker was approximated to be cylindrical. The vessel was filled to the height l. The make-up of the steaming vessel was estimated to be 1 mm stainless steel type 1.4301 [36], the volume of the vessel to be 6 m^3. The vessel was not insulated. Heat transmission $\dot{q}_{tr}$ of the fluid filled area was calculated as follows:

$$\dot{q}_{tr,li} = \frac{2 \cdot \pi \cdot l \cdot (\vartheta_{in} - \vartheta_{out})}{\frac{1}{r_{in} \cdot \alpha_{in,li}} + \frac{\ln\left(\frac{r_{out}}{r_{in}}\right)}{\lambda_s} + \frac{1}{r_{out} \cdot \alpha_{out,li}}} \quad (4)$$

With

$$l = \frac{V_{mix}}{\pi \cdot r^2} \quad (5)$$

And

$$V_{mix} = (m_w \rho_w + m_{sb} \rho_{sb} + m_{wg} \rho_{wg} + m_{wb} \rho_{wb}) \quad (6)$$

For the calculation of the heat transmission of the gas filled area $\dot{q}_{tr,ga}$, $\alpha_{in,li}$ was replaced by $\alpha_{in,ga}$.

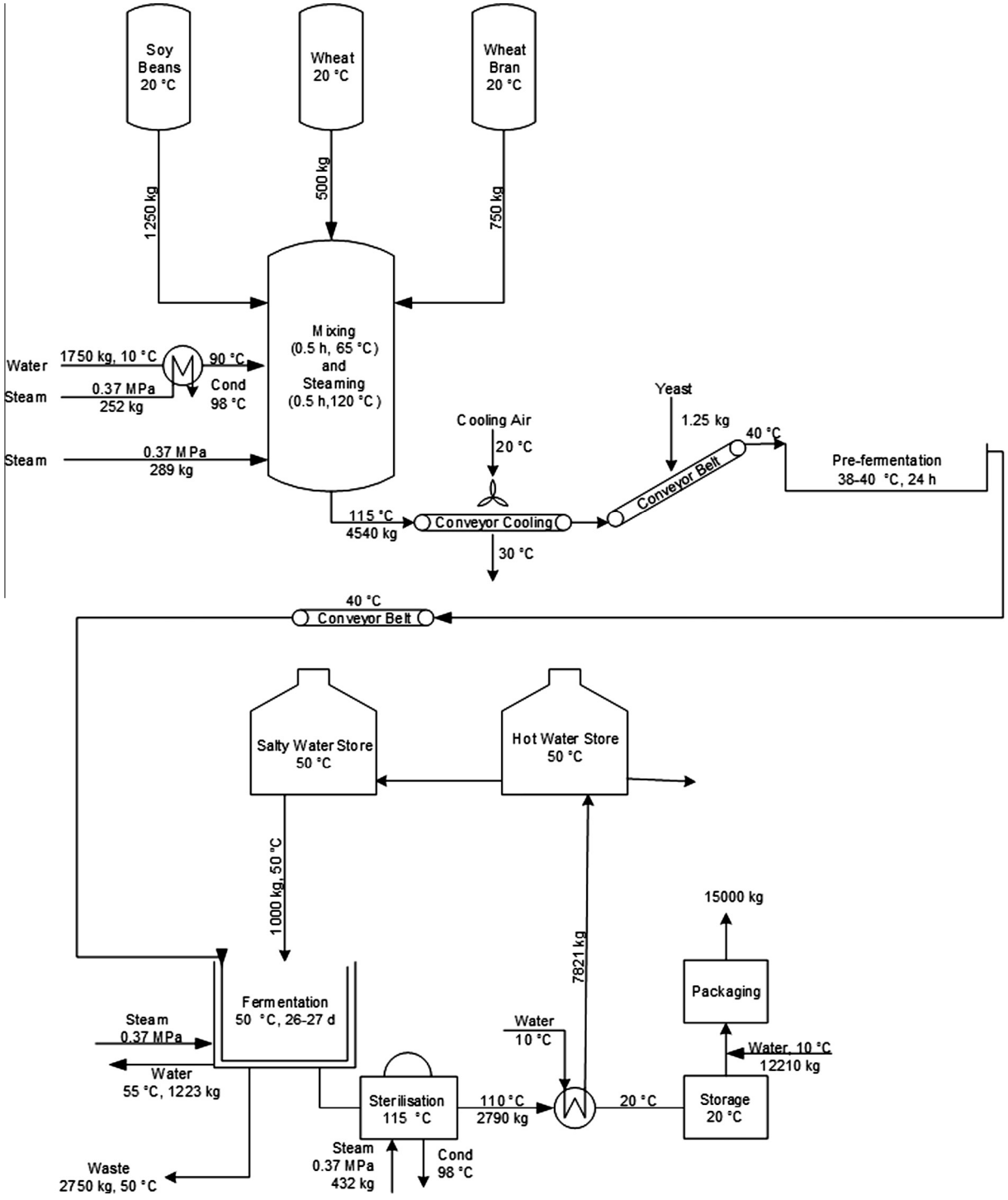

Fig. 1. Process flow diagram.

The heat transmission at the bottom $\dot{q}_{tr,b}$ was calculated using:

$$\dot{q}_{tr,b} = \frac{A \cdot (\vartheta_{in} - \vartheta_{out})}{\frac{1}{\alpha_{in,li}} + \frac{s_s}{\lambda_s} + \frac{1}{\alpha_{out,li}}} \quad (7)$$

For the calculation of the heat transmission of the top $\dot{q}_{tr,t}$, $\alpha_{in,li}$ was replaced by $\alpha_{in,ga}$.

For the calculation of heat losses towards the air in the convective cooling stage Eq. (3) was used. It was assumed that the material is thinly enough distributed on the conveyor belt to reach a uniform end temperature of 40 °C and only transferred thermal energy, but no water, to the air. Minimum air demand was calculated using 20 °C surrounding temperature and a final air temperature of 30 °C as given by the production manager.

3.1.3. Fermentation stage

The dimensions of the fermentation vats are 3.5 × 2.0 × 2.15 m. The vessels were assumed to consist of 1.5 mm stainless steel type 1.4301 [36]. For the heat loss calculations of the vats, heating with steam at 152 °C was assumed. As the vats are not covered, the heat losses towards the room were calculated using natural convection

towards the air, with a convective heat transfer coefficient of 10.45 W/m^2 K and a surface temperature of 50 °C. The area exposed to the surroundings was 7 m^2. It was assumed that no heat was lost through the water baths. The only losses accounted for were the losses from the surface of the mix, assuming a uniform product temperature of 50 °C. Calculations were conducted using Eq. (8):

$$\dot{q}_{tr,v} = A \cdot k_{mix} \cdot \Delta\vartheta \tag{8}$$

Heat losses through the water leaving the system at 50 °C were calculated with Eq. (2).

The dimension of each production hall is 40.0 × 37.5 × 7.0 m (10,500 m^3). Each fermentation room borders other rooms on three sides which are heated to the same temperature, thus only the outer wall and the roof were considered in the heat loss calculations. The outer wall also has a glass front consisting of single glassed panels. A single glass front with the dimensions of 1.25 × 35.0 m was assumed. The construction material was assumed to be 30 cm poured concrete for the walls, a vertical single glassed window and the roof to consist of 5 cm concrete slab and 2.5 cm insulation with heat transfer coefficients of 5.8, 5.9 and 0.9 W/m^2 K respectively. The heat losses through the wall were calculated as:

$$\dot{q}_{tr,wall} = \left(\frac{A_{conc}}{\frac{1}{k_{conc}}} + \frac{A_{gl}}{\frac{1}{k_{gl}}}\right) \cdot (\vartheta_{in} - \vartheta_{out}) \tag{9}$$

The heat losses through the roof were calculated using:

$$\dot{q}_{tr,roof} = \left(\frac{A_{roof}}{\frac{1}{\alpha_{in}} + \frac{s_{ins}}{\lambda_{ins}} + \frac{s_{conc}}{\lambda_{conc}} + \frac{1}{\alpha_{out}}}\right) \cdot (\vartheta_{in} - \vartheta_{out}) \tag{10}$$

For the heat loss calculations towards the surroundings, the average monthly ambient temperatures of Beijing for the year 2011 were used as displayed in Fig. 2, generated using Meteonorm 6 software. The year 2011 was chosen as the company was able to provide the most complete data for this year.

According to the production manager, the temperature in the heating phase (October to March) is kept at a minimum of 15 °C. However, it is highly likely that in reality, with the installed system, keeping these temperatures is not possible. This could not be further investigated as the room temperature is not recorded and the site visits were conducted in September.

For the calculation of the room heating demand, the following assumptions were made: the heating is only turned on when the room temperature falls below 15 °C, for those periods the heating demand was calculated using the monthly average as given in Fig. 2. For a more accurate result, daily or even hourly temperatures would have to be used. Heat loss calculations for the condensate were conducted using Eq. (3).

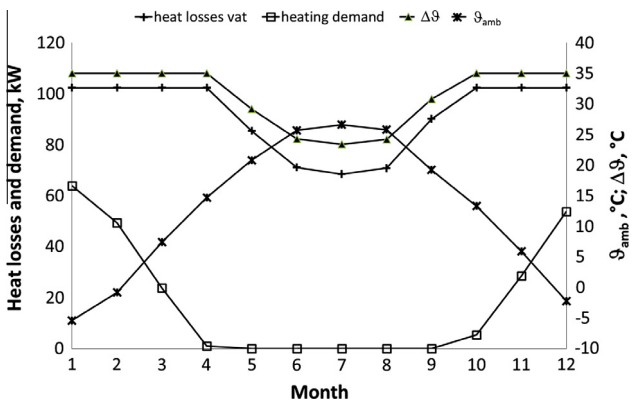

Fig. 2. Average ambient temperature, heat losses from vats, room heating demand and temperature difference between product surface and room temperature.

Heat losses through discarding of the solid waste had to be based on assumptions as there were no data on amounts and composition available. Information from the brewing sector was used, where brewer's grain is considered 1.1–1.3 kg per kg of malt at a moisture content of 80% [37]. Initial moisture contents of the soy and grain was estimated to be 0.13 kg/kg which is the industrial standard for dried grains. This leads to a total ratio of dry residue of 25%. Thermal properties of dry residue were assumed to be identical to the raw ingredients.

$$Q_{wa} = 0.8 \cdot m_{wa} \cdot c_{p,w} + 0.2 \cdot m_{wa} \cdot c_{p,mix} \tag{11}$$

with

$$m_{wa} = m_w + m_{so} = (m_{sb} + m_{wb} + m_{wg}) \cdot 1.1 \tag{12}$$

3.1.4. Sterilisation stage

Heat demand during sterilisation was calculated using Eq. (3), utilising the specific heat capacity of soy sauce as displayed in Section 3.1.2. Sterilisation was conducted under pressure at 115 °C, therefore no evaporation occurred.

3.1.5. General assumptions made

The calculations carried out were based on full utilisation of all vats throughout the year based on optimum scheduling. This translates to 281 production days or 2246 batches. However, as shown in Table 1, production rates fluctuate significantly and adjust to the market demands continuously.

3.2. Process optimisation and heat integration

The reduction of heat demands is split into two parts, the UO optimisation and the process integration. Recent studies have shown that a change of processing technologies can lead to significant reductions of energy demands [38]. New technologies offer different opportunities for integration; therefore, it is essential to undertake changes in the UOs before integrating the system. In the integration step available, heat recovery potentials within the utilities (supply of heat, cold, and compressed air) are evaluated.

Due to the physical system set up and the production scheduling, classic pinch analysis could not be applied. These restrictions extended to the introduction of new technologies for the UOs involved. The suggestions for process integration developed were based on the location of heat sources and sinks and their individual timings. Calculations were based on the availability of waste heat and the demand in the source streams. The minimum temperature difference of 10 °C between source outlet and sink inlet in the heat exchangers was used because this is industrial standard. Depending on the location of the waste heat streams and their use, two different approaches had to be chosen.

Table 1
Production data overview.

		2008	2009	2010	2011
Ratio Soy Sauce (RS)	%	0.87	0.91	0.81	0.81
Ratio Vinegar (RV)	%	0.13	0.09	0.19	0.19
Specific Steam Demand (SSD)	$t_{steam}/t_{product}$	1.86	0.88	0.67	0.66
Specific Total Energy Consumption (SEC)	$t_{coalequ}$	0.16	0.10	0.07	0.07
Relative energy consumption (REC)	%	0.88	0.79	0.92	1.00
Specific water demand (SWD)	m^3/m^3	2.95	3.28	2.43	2.32
Relative costs per unit (RCU)	%	0.59	0.92	0.94	1.00

In the first scenario, heat was recovered from the soy sauce after sterilisation. Cold water with an inlet temperature of 10 °C was pre-heated to 50 °C for the use as process water. Under these circumstances, the heat sink was available immediately and until the end of the availability of the waste heat. The soy sauce exited the steriliser at 110 °C and was cooled to 20 °C. Therefore, the following approach was chosen:

$$Q_r = m_{ss} \cdot c_{p,ss} \cdot \Delta\vartheta_{ss} \tag{13}$$

And the mass of water heated was

$$m_w = \frac{Q_r}{c_{p,w} \cdot \Delta\vartheta_w} \tag{14}$$

In the second scenario, for the condensate from the water pre-heating in the mixing stage and the sterilisation, a different approach had to be chosen. In both cases, the waste heat is only available after a certain proportion of the medium to be heated (water or soy sauce) has already been heated. Accordingly, the last proportion of the recovered heat cannot be utilised as there is no heat sink available. Water entered the system at 10 °C and soy sauce at 50 °C, condensate temperature was at 98 °C. Calculations were conducted using Eq. (15)

$$Q_r = \int (m_w \cdot c_{p,w} \cdot \Delta\vartheta; t; t_1; t_{n-1}) \tag{15}$$

The amount of un-utilised waste heat was calculated using

$$Q_l = Q_{wh} - Q_r \tag{16}$$

With

$$Q_{wh} = \int (m_w \cdot c_{p,w} \cdot \Delta\vartheta; t; t_0; t_n) \tag{17}$$

3.3. Integration of solar process heat

The energy demands for heating and cooling on a considered site varies significantly with location, time of the day and period of the year [28] and, in the present case, on the current market demand. For illustration of dependencies, Fig. 3 shows a comparison of systems in Beijing and 5 other locations relating to direct normal irradiation (DNI), gross heat production (GHP) and the yearly average efficiency of a solar thermal system producing 2 t/h of steam (ca. 6000 m^2 collector size), utilising Fresnel collectors, installed flat and orientated East–West. Calculations were provided by Industrial Solar GmbH company, a provider of a Fresnel solar concentrating collector, using their internal collector performance model. Clearly, the level of DNI (direct normal insolation) plays a significant role towards the yearly efficiency, especially for concentrating collectors and therefore determines the sizing of the system.

3.3.1. Simulation description

To determine the performance of both a photovoltaic (PV) and solar thermal (ST) plant, an hourly year-long simulation was conducted in MATLAB for two solar integration points: batch heating of the inlet water and other ingredients from 10 °C to 90 °C (Mixing) and the creation of saturated steam (from 10 °C) at 0.37 MPa for the second cooking (Steaming) process. The hourly energy yield of the selected solar panels was calculated in accordance to Duffie and Beckman [39] for solar thermal collectors ($\dot{Q}_{ST}$) (Eqs. (18) and (19)) and photovoltaic collectors ($\dot{Q}_{PV}$) (Eq. (21)), and modified with a system efficiency term which encompasses both thermal losses from the storage tanks and required heat exchanges. Meteorological data was obtained by the METEONORM database, which provided the available solar radiation (H_t) at a collector tilt angle, ambient temperature (ϑ_a) and beam incident angles on the collectors (θ), required to calculate the Incident Angle Modified (AM). The PV efficiency (η_{PV}) was set at 17% with a system efficiency $\left(\eta_{sys}^{PV}\right)$ of 90%. The Area (A) was held constant at one square metre to calculate the specific annual energy yield $\left(\bar{Y}_{1,2}^{ST,PV},\ [\mathrm{kW\,h/m^2\,a}]\right)$ which was beneficial for the next section. Values and explanations of the remaining symbols are found in Table 2.

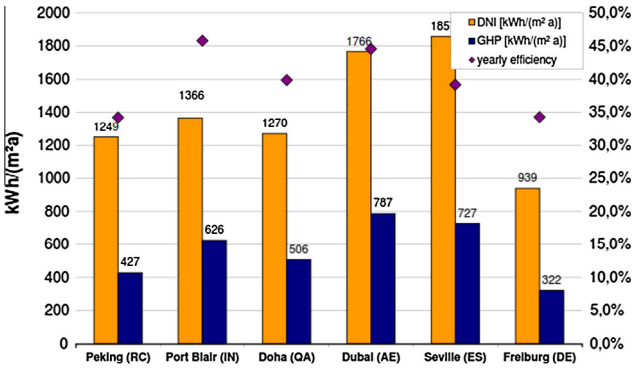

Fig. 3. DNI, GHP and yearly efficiency of evacuated tube collectors for different locations [Industrial Solar GmbH; personal correspondence].

Table 2
Simulation parameters of the solar thermal collectors.

		Case 1 – mixing	Case 2 – steaming	
		Flat plate	Vacuum Flat Plate	Flat plate and PV
Optical coefficient	η_0	0.871	0.759	0.871
Linear Thermal Loss Coefficient (W/m^2 k)	a_1	3.162	0.508	3.162
Quadratic thermal loss coefficient (W/m^2 k^2)	a_2	0.0018	0.007	0.0018
Inlet temperature (°C)	ϑ_i	20	140	10
Outlet temperature (°C)	ϑ_o	100	190	140
System efficiency (%)	η_{sys}^{ST}	85	85	87.5

$$\dot{Q}_{ST} = A * H_t * \mathrm{IAM} * \left(\eta_0 - \frac{a_1\left(\frac{\vartheta_o+\vartheta_i}{2} - \vartheta_a\right)}{H_t} - \frac{a_2\left(\frac{\vartheta_o+\vartheta_i}{2} - \vartheta_a\right)^2}{H_t}\right) * \eta_{sys}^{ST} \tag{18}$$

$$\mathrm{IAM} = 1 - 0.1 * \left(\frac{1}{\cos^{-1}\theta} - 1\right) \tag{19}$$

$$\dot{Q}_{PV} = A * H_t * \mathrm{IAM} * \eta_{PV} * \eta_{sys}^{PV} \tag{20}$$

The collectors were facing south and tilted to 40°, the latitude of Beijing, which was chosen to give the highest annual yield [40]. An efficient flat plate was selected for the lower temperature applications and a higher performing Vacuum Flat Plate for higher temperatures. A concentrated thermal collector (i.e. parabolic-trough [41–43]) was not selected for this comparison due to relatively low DNI values as a result of a high concentration of atmospheric aerosols. Thermal energy storage was needed to buffer not only the transient solar radiation and respective thermal yield, but also to compensate for the intermittent batch processes during the day. Both a thermocline hot water storage tank and a steam drum were included in the model, along with thermal losses though the heat exchanges, represented collectively by a "System Efficiency $\left(\eta_{sys}^{ST}\right)$" term, which was validated through the prior works of

Lauterbach [44] and PVWatts. The results of these simulations are found in Section 4.4.

3.3.2. Solar project sizing

The size of each plant was constrained by two main factors: the available rooftop space on the building (~5000 m^2); and the peak daily hot water and steam demand (1300 kW h/d $[D_1^p]$ and 1730 kW h/d $[D_2^p]$, respectively), excluding the random heating of the fermentation tanks and sterilization process. Sizing of the respective solar heating plants was done in accordance to VDI 6002 [45] and extended by Lauterbach [44]. In these documents, it was recommended to avoid wasting thermal energy by designing the solar plant to meet the peak demand in the summer. This was done by first conducting an annual simulation as above on one square metre of collector, whether flat plate, Vacuum Flat Plate, or Photovoltaic in order to determine the annual specific yield $\left(\bar{Y}_{1,2}^{ST,PV},\ \text{kW h/m}^2\ \text{a}\right)$, as described in Section 3.3.1. Then, the annual yield $\left(\text{Yield}_{1,2}^{ST,PV}\right)$ for the entire solar system could quickly be determined once the collector areas $\left(\text{Area}_{1,2}^{ST,PV},\ \text{m}^2\right)$ was known.

$$\text{Yield}_{1,2}^{PV,ST} = \text{Area}_{1,2}^{ST,PV} * \bar{Y}_{1,2}^{ST,PV} \tag{21}$$

The solar collector area for a desired process is determined by dividing the daily demand of said process ($D_{1,2}^p$, kW h/d) by the highest daily specific output of said collector, ($S_{1,2}^{ST,PV}$, kW h/m^2 d), commonly referred to by VDI 6002 [24] and Lauterbach [44] as a "Good Solar Day." This day and value was determined by condensing the hourly to a daily annual specific yield, which the highest day denoted as such $\left(S_{1,2}^{ST,PV}\right)$.

$$\text{Area}_{1,2}^{ST,PV} = \frac{D_{1,2}^p}{S_{1,2}^{ST,PV}} \tag{22}$$

An example of the "Good Solar Day" $\left(S_1^{ST,PV}\right)$, circled, are shown below in Fig. 4 for the Mixing case, provided from MATLAB simulations described in Section 3.3.1. The Specific Annual Yield $\left(\bar{Y}_1^{ST,PV}\right)$ is the summation of the Specific Daily Yields throughout the year. Using these values and Eqs. (21) and (22), the performance of the solar plants to meet the required thermal demand in Mixing and Steaming cases can be calculated.

3.4. Economic appraisal

Two key financial parameters were calculated to determine if a project is financially feasible, the Levelised Cost of Energy (LCOE) and Payback Period. The LCOE equation for the solar projects is show in (Eq. (23)), including the project lifetime (L), operations and maintenance costs (O&M), depreciation rate (DR) and system degradation rate (SD). Project costs ($\text{Cost}_{ST,PV}$) were derived from the specific installed collector cost in Table 3, multiplied by the size of the project, determined in Table 5, where the $\text{Yield}_{1,2}^{PV,ST}$ is also listed.

$$\text{LCOE} = \frac{\text{Cost}_{ST,PV} + \sum_{n=1}^{L} \frac{\text{OM}}{(1+\text{DR})^n}}{\sum_{n=1}^{L} \frac{\text{Yield}_{1,2}^{PV,ST} * (1-\text{SD})^n}{(1+\text{DR})^n}} \tag{23}$$

The Payback Period is the point when the energy generated by the solar system, valued at the cost of fuel (or network steam in this case), surpasses the sum of its upfront costs and annual O&M. The cost and revenue flows of the solar projects were evaluated at the end of each year and, when the value of the project changes from negative to positive, the Payback Period is determined.

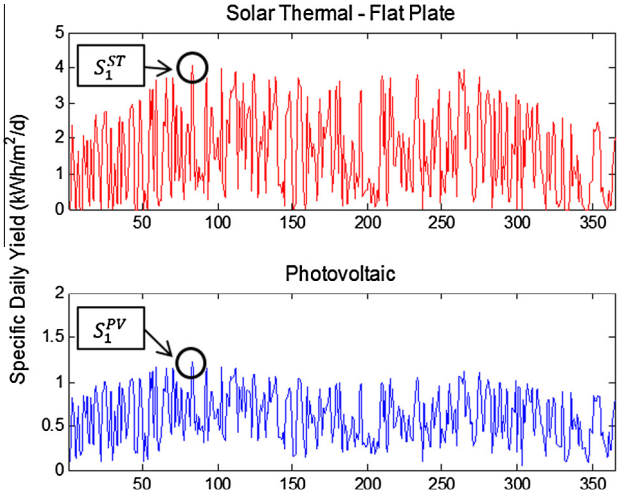

Fig. 4. Simulation results for the ST flat plate and PV collectors in case 1 (Mixing). The circled points indicate the "Good Solar Day" for both cases. The integration of the graphs provides the specific annual yield of the collectors in Beijing.

Table 3
Simulation input parameters.

Parameter	Value	Unit	Source
Flat plate collector	2051	Yuan/m^2	[48]
Vacuum flat plate collector	3420	Yuan/m^2	[48]
PV panels	11.62	Yuan/W_p	[49]
Degradation rate (DR) of ST	1	%	[50]
Degradation rate (DR) of PV	1	%	[51]
System lifetime (L)	20	Years	[51]
operation and management (O&M)	1.5	% of installed	[51]
discount rate (DR)	3.17	%	[46]
Steam price	0.31	Yuan/kWh	[47]
inflation rate of steam/electricity	5	%	[47]

For the evaluation of energy price developments an inflation rate of 3.14% was used, which is the average annual inflation rates from 2008 to 2012 [46]. The steam price used for the estimation of the financial benefit of implementation of solar thermal installation was taken from the Chinese Governmental website [47] and is at 230 Yuan/t, or 0.31 Yuan/kW h (0.045 €/kW h), subject to a 5% inflation rate. It was assumed that the company would self-finance this project and not borrow money from a lending agency. The prices for the solar thermal steam system and its installation were based on three case studies carried out by Shanghai Jiao Tong University [48]. A summary of the input parameters for the analysis are exhibited in Table 3. Results of the economic comparison are shown in Section 4.4.

4. Results

4.1. System analysis based on energy and water bills

The most important production data for the course of 2008–2011 are displayed in Table 1. Throughout the regarded period, the ratio of soy sauce production (RSS) had always by far outweighed vinegar production (RV). However, before the modernisation of the vinegar production line in May 2009 (Fig. 5), its contribution to the energy demand was enormous, which is directly reflected in the average Specific Steam Demand (SSD) and the resulting Specific Total Energy Consumption (SEC), which was more than twice as high before than after the modernisation.

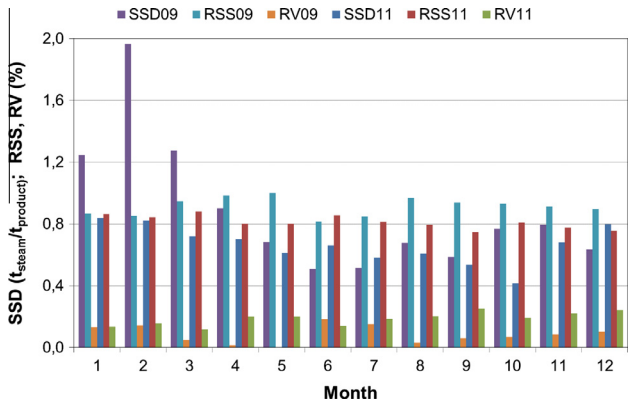

Fig. 5. Saturated steam demand, Ratio Soy Sauce and Ratio Vinegar as a function of time of the year for 2009 and 2011.

The specific water demand (SWD) also reduced after the refurbishment, however, it is not entirely clear what caused the rise in 2009. One of the influential factors on SWD is the ratio between 1st, 2nd and 3rd class soy sauce. The 1st class product contains no additional water and different amounts of additional water are used for the 2nd and 3rd class products, which are added directly before packaging. On average, 4.4 kg of water is added for every kg of product after sterilisation. The relative costs per unit (RCU), which are the ratio between the actual energy costs at the time and the costs in 2011 (with consideration of inflation), show how drastically energy prices rose with the economic crisis in 2009, with a level of 59% in 2008 and 92% in 2009.

Fig. 5 depicts the development of SSD, RSS and RV on a monthly basis for 2009 and 2011. The effect of changes in the vinegar production can be clearly seen by the drop of specific energy demand between January 2009 and June 2009. The peak in February, and the still very high SSD in March despite the low percentage of vinegar production, cannot however be explained by very cold weather conditions as January was reportedly the coldest month and had similarly high production levels as February. The fact that the specific energy demands do not follow clear seasonal tendencies can be explained as: firstly, vinegar production is less energy intensive than soy sauce production, so an increase in the RV will result in a decrease in the SSD. Secondly, for 2nd and 3rd class soy sauce, the additional water is only added after the production, therefore in these cases the specific SSD is lower than for 1st class produce.

4.2. Process audit and evaluation

The processing is carried out as described in Section 2.2 (Fig. 1). Table 4 gives an overview of all energy demands, direct heat losses and heat losses through discarding the condensate.

In the cooking stage, heat is lost due to the lack of insulation of the steaming vessel. In the transfer phase, where the product is cooled to 40 °C using forced air, in average 255 kW h of heat are lost per batch produced. Annually, in the region of 572 MW h are lost this way. There is no technologically feasible way of recovering this heat.

The pre-fermentation takes place at a temperature of 40 °C in an enclosed room, which is, when necessary, heated with conventional radiators. Heat losses here are minimal due to the small size of the room the short time the product is staying there and the fact that the room itself is enclosed in a bigger room which is additionally insulated. By far the highest losses occur in the actual fermentation phase. This is due to vessels that are open to the surroundings, in which the product needs to be kept at 50 °C, as well as a room of 10,500 m^3 volume, with a large glass front and uninsulated walls, which needs to be kept at a minimum of 15 °C even in winter. Fig. 2 shows the interrelation of ambient temperature, temperature difference between the vats and the room temperature, heat losses through the product surface in the vats (values for 40 vats) and heating demand. The heat losses from the vats into the surrounding air were calculated to be 804 MW h/a (1.6 GW h/a), whilst the total heating demand for room heating sums up to 164 MW h/a (328 MW h/a).

The waste is discarded of at a temperature of 50 °C and consists of 80% water and 20% dry matter. 85 kW h of heat are lost per batch with the waste. This translates to 191 MW h/a of heat losses.

The overall non-recovered theoretical heat losses amount to 1.3 MW h per batch and would sum up to 3.0 GWh/a at full utilisation.

4.3. Potentials for heat recovery and process integration

In addition to the already existing waste heat recovery in the sterilisation stage, two easily applicable integration points were identified in waste heat recovery from condensate in the mixing/cooking and sterilisation steps. Firstly, the heat from condensate in the water pre-heating before mixing could be used to pre-heat the water flow from 10 °C to 29 °C. This would amount to a reduction of energy demand in this step by 13% or 23 kW h/batch. Secondly, the condensate from the sterilisation process could be used to pre-heat the soy sauce before entering the steriliser from 50 °C to 62 °C. This would lead to a reduction of energy demand by 14% or 39 kW h/batch. However, these two measures would only account for reductions in the overall energy demand by 4.5%.

Due to the nature of the system, beyond these two measures, theoretically only the room heating system could be supplied with heat at temperature levels below 100 °C; however, an underfloor heating system could not be implemented as there is no room for such measures. Therefore, a new radiator system would have to be installed. However, in total, the energy demand for room heating only makes up 17% of the total theoretical heat demand

Table 4
Energy demands, direct and indirect heat losses for the production line by batch and as a yearly total.

Process step		Energy demand [kW h]	Recovery [kW h]	Heat losses process [kW h]	Heat losses condensate [kW h]
Heating of mix		171	–	4	23
Steaming		176	–	12	–
Convection cooling		–	–	255	–
Pre fermentation		11	–	11	–
Fermentation heating		35	–	–	2
Fermentation (maintenance of temperature)	Min	555	–	555	39
	Max	799	–	799	56
	Average	716	–	716	50
Solid waste				85	–
Sterilisation		280	360	20	39
Batch total		1354	360	1102	208
Yearly total		3,041,465	808,728	2,475,977	467,684

and is only required from November until March (Fig. 2), when solar irradiation is the lowest. Thus, this type of investment could not be justified. Technologically, the required heating demand could easily be reduced by the reduction of the total volume of the hall that needs to be heated through the introduction of suspended ceilings. This would have the additional advantage that up to date insulation could be introduced into the ceiling, further reducing the energy demands. Another technologically feasible option would be the introduction of lids on the vats. However, the auditors were told that this was not an option due to the threat of negatively influencing product quality. Therefore this option was not considered.

Beyond the above described and already installed measures there is no scope for further integration of the current system.

4.4. Integration of solar PV and thermal heat, financial appraisal

Through the analysis, feasible systems were designed which could meet a significant amount of the energy demand for the mixing and steaming of soy sauce ingredients. Interesting results emerged, showing that at lower temperatures, solar thermal collectors prove to be more cost effective, while at higher temperatures, PV collectors used for steam generation prove to be a slightly better investment when directly compared to their thermal counterpart. In depth results are show below.

4.4.1. Simulation results

The simulation, as described in Section 3.3.1, provided the hourly performance of the solar collectors. When integrated over the year, the Annual Specific Solar Yield $\left(\bar{Y}_{1,2}^{ST,PV}\right)$ was determined, noted in Table 5. As typically seen in solar thermal projects, lower temperature applications generally have a higher $\bar{Y}$ since thermal losses are less, which was confirmed here. Case 1 $(\bar{Y}_1^{ST})$ yielded 589 kW h/m^2 a, nearly doubling that of Case 2 $(\bar{Y}_2^{ST})$ at 336 kW h/m^2 a. PV generated heat $\left(\bar{Y}_{1,2}^{PV}\right)$, in both cases produced equal amounts energy, since the electrical heating process was insensitive to operating temperature. The Cascade system in Case 2 provided a slightly higher value at 233 kW h/m^2 a, indicating a potential benefit as compared to other systems generating steam. Also determined from this simulation was the "Good Solar Day Yield" $\left(S_{1,2}^{ST,PV}\right)$, whose comparative results were similar to the Annual Yield (Table 5), and necessary to size the solar projects to meet the demand. By dividing the Daily Process Demand $\left(D_{1,2}^{p}\right)$ by $\left(S_{1,2}^{ST,PV}\right)$, the required collector area for the project was determined (Eq. (22)). For Case 1, 319 m^2 of flat plate collectors are required to meet the Mixing demand, as shown below. The other calculated collector field sizes are found in (Table 5).

$$\text{Area}_1^{ST} = \frac{D_1^p}{S_1^{ST}} = \frac{1300\,\frac{\text{kW h}}{\text{d}}}{4.07\,\frac{\text{kW h}}{\text{m}^2\,\text{d}}} = 319\ \text{m}^2$$

The calculation of the annual energy yield follows Eq. (21), by multiplying the $\text{Area}_{1,2}^{ST,PV}$ by the Annual Specific Solar Yield $\left(\bar{Y}_{1,2}^{ST,PV}\right)$. Following the solar thermal field in Case 1, this system will produce 188 MW h of thermal energy at 90 °C per year, shown below, with the other cases' yield displayed in Table 5.

$$\text{Yield}_{1,2}^{PV,ST} = \text{Area}_{1,2}^{ST,PV} \cdot \bar{Y}_{1,2}^{ST,PV} = 319\ \text{m}^2 \cdot 589\,\frac{\text{kW h}}{\text{m}^2\,\text{a}} = 188\,\frac{\text{MW h}}{\text{a}}$$

One other project constraint was the limited rooftop space at 5000 m^2. To estimate the required rooftop space for these solar projects, a footprint of 2.5 times greater than the installed collector area was assumed [52]. All of the systems were well below this limit, though the steam generating PV system did take up the largest amount of space at 3571 m^2.

Table 5
Summary of yields for heating and steam generation cases.

	Case 1 – heating		Case 2 – steam generation		
	Solar thermal	PV	Solar thermal	PV	ST + PV cascade
Annual Specific Solar Yield (kW h/m^2/a) $\left(\bar{Y}_{1,2}^{ST,PV}\right)$	589	221	336	221	233.30
Good Solar Day Yield (kW h/m^2/d) $\left(S_{1,2}^{ST,PV}\right)$	4.07	1.21	2.91	1.21	1.39
Solar field size (m^2) $\left(\text{Area}_{1,2}^{ST,PV}\right)$	319	1073	595	1429	1245 (100 ST, 1145 PV)
Annual energy yield (MW h/a) $\left(\text{Yield}_{1,2}^{PV,ST}\right)$	188	236	200	316	290
Rooftop space (m^2)	721	2684	1486	3571	3112

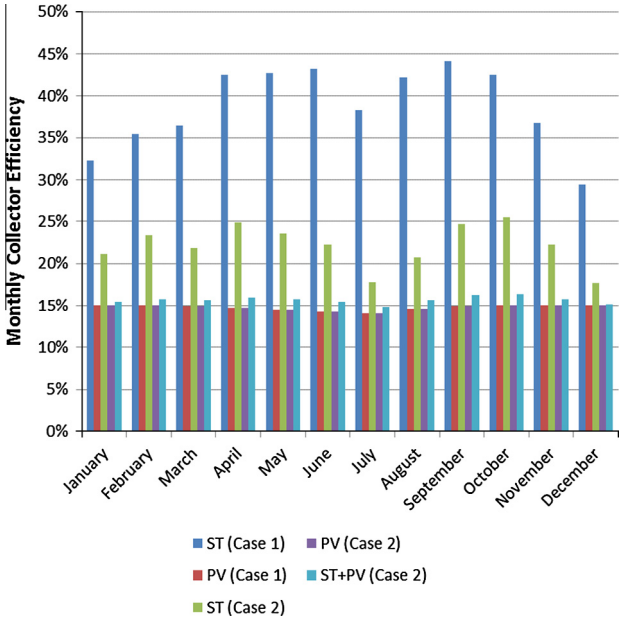

Fig. 6. A monthly specific collector yield for the two simulation test cases and five collector field configurations.

For the Cascade system in Case 2, flat plate collectors heated water from 10 °C…140 °C and the PV collectors boosted this stream to saturated steam at 152 °C, leading to 9% FP and 91% PV by collector surface area. These annual yields and solar field sizes were used as inputs for the financial comparison in Section 4.4.2.

It is interesting to note that while all systems were sized to meet the daily demand for their "Good Solar Day," the PV systems, though less efficient, produced significantly higher annual yields. This was due to the thermal losses which occurred in solar thermal collectors, giving them fewer productive hours over the year to produce energy. Since the PV collectors are not affected by this, they will produce more annual energy.

The simulation results displayed in Fig. 6 show the average monthly efficiency of the 5 solar systems. The ST system in Case 1 clearly converts solar radiation at the highest efficiency, followed by the ST system in Case 2. Both of these collectors are affected by

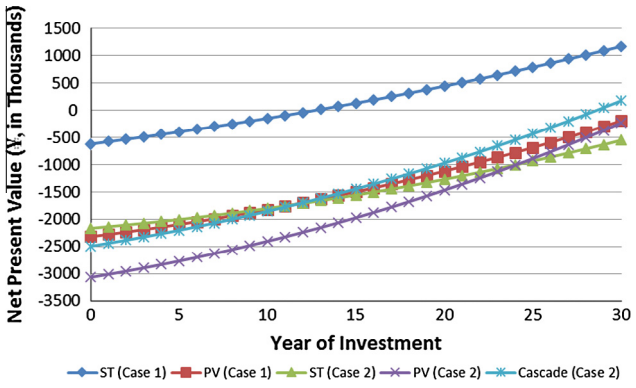

Fig. 7. The Net Present Value of the solar systems.

the ambient temperatures in Beijing, showing the lowest efficiency during the winter months. More consistent are the PV collectors in both cases, which generally exhibit an average efficiency of 15% but decrease slightly in the summer. This was mainly caused by the increase in the IAM due to the collector tilt angle set at Beijing's latitude. While this graph is helpful to understand how efficient the systems are over the year, the overall energy cost will determine which project should be installed. Results of the financial analysis are shown in Section 4.4.2.

4.4.2. Financial analysis

To pre-heat water to 90 °C for Case 1, the solar thermal system produced energy at a cost of 0.063 €/kW h with a payback time of approximately 13 years (Fig. 7), observed when the dark blue line passes from a negative Net Present Value (NPV) to a positive. In comparison, the PV system heated water at a rate of 0.159 €/kW h, with no foreseeable payback period within the assumed 20 year lifetime of the system (red[1] line of Fig. 7). While generous tariffs are available for grid fed-in PV generated electricity (up to 1 Yuan/kW h (0.146 €/kW h)) [30], they do not apply in this case as all generated electricity is internally consumed.

Steam generation produced antipodal results as compared to Case 1. The cost per kW h of generated steam remained the same for the PV system (1.08 Yuan (0.159 €)), but the cost from solar thermal generation increased significantly to (1.223 Yuan (0.18 €)/kW h), due to the high operating temperatures (i.e. lower system efficiency) and more expensive collectors. The lowest cost for steam generation was produced by the Cascade system, reducing the PV generated steam cost by 10% to 0.985 Yuan (0.145 €)/kW h. All three systems however did not achieve a payback period within the 20 year project horizon (Fig. 7). If a 30 year timeline was assumed for the projects, then the Cascade system for Case 2 would hit its payback time in the 29th year.

It should be noted that this current financial analysis did not incorporate local incentives for solar generated energy for two reasons. First, the majority of incentives for solar heat generation are focused towards domestic hot water systems, which did not apply in this case. This is also coupled with the fact that most solar thermal incentives are now being phased out of China, due to an increasing interest in PV rooftop applications thus generating competition for rooftop space. Second, for PV, was that these systems would not qualify for the Feed-In-Tariff schemes commonly found throughout China, since the generated energy is not fed to the grid. Had an Investment Tax Credit been available instead, financial feasibility would have been more obtainable.

[1] For interpretation of color in Fig. 7, the reader is referred to the web version of this article.

5. Discussion

The energy audit conducted revealed significant amounts of waste heat produced along the whole production process of which the company had not been aware. Due to the lack of in process monitoring and recording, as well as the availability of energy data only on a total site level, which included a vinegar plant alongside the soy sauce plant energy, the production manager had not been in a position to reliably evaluate the current situation before the conducted audit. The only existing energy integration point at the time of the audit had been the heat recovery from the sterilisation stage. This is state of the art in most food producing companies.

The vast majority of waste heat cannot be utilised within the current system set up. Furthermore, the production engineer does not want any intrusive measures to be taken as he does not want to risk a change in the taste of the product. This is particularly important as the change in the vinegar production led to a significant loss in the market share. Only two very easy to implement measures were identified that could be realised.

The energetic simulations of the solar heat generation produced the expected results due to input parameters. Traditional flat plate collectors are extremely efficient at lower temperatures and should be the preferred choice for such applications, as their performance to cost ratio is relatively high. This is clearly evident in the wide spread adaptation of solar thermal domestic hot water systems within China. PV should never be used for the heating of domestic hot water as there is no economic justification. For higher temperatures, Beijing was a unique case due to the reasonably good levels of GHI, but rather low levels of DNI due to frequent smog and haze, a result of local pollution stemming predominantly from coal based electricity and heat generation.

Due to this, a concentrating thermal collector was avoided (which is typically used for steam generation) and a Vacuum Flat Plate collector used in its place. There was a significant thermal penalty incurred from this selection, as the radiation losses were quite high due to the high operating temperatures (Mean Plate Temperature = 172.5 °C), and the large collector surface area. With a concentrating collector, these losses are minimized due to a very small collector surface area (10–20 times smaller; i.e. 10–20 times fewer thermal losses), and thus perform better at higher temperatures with ample DNI resources. Due to these factors, cost effective solar thermal generation of steam was at a disadvantage due to the large fraction of diffuse radiation. This supports the generally accepted practice that projects demanding high processes temperatures, in high solar radiation locations, should rely on concentrating technologies. Following this, the research presented here gives indications that in lower to medium solar radiation regions where steam is desired, PV based steam generation (especially coupled with low cost ST for pre-heating) is becoming increasingly economically feasible. With the prices for PV expected to be continually decreasing, this is only the starting point for PV based steam generation for industrial applications.

It should be noted that the export (or internal consumption) of PV generated electricity is normally more financially feasible as compared to electrical heating. The authors are aware of this and, for most applications, solar generated electricity should only be used for electrical demands, and thermal for thermal. However, in regions where net metering is not allowed (Mississippi, South Dakota, and Tennessee in the United States, for example), PV use for electrical heating may provide a better technical solution. It

was the intent of the authors to directly compare these two technologies for heat generation.

6. Conclusions

The aim of this study was the evaluation of the feasibility of waste heat recovery, process integration and introduction of renewable energy sources in the form of solar heat generation in a soy sauce plant in the greater Beijing area. It was found that only about 5% (138 MW h/a) of the currently unutilised waste heat can be technologically feasibly recovered. Beyond this, scheduling issues, structural constraints within the system, costs for retrofitting and reluctance to change the process due to the potential impacts on product quality act preventive to further modifications of the system.

Simulations of several scenarios for solar heat production have shown, that the integration of solar thermal energy for both, hot water and steam generation are feasible. Provision of hot water in the cooking stage of 170 MW h/a at a 20 years LCOE of 0.063 €/kW h was analysed. Steam generation for the steaming process was most cost effective with a cascade system of PV and flat plate collectors delivering 290 MW h/a with an estimated 20 year LCOE of 0.145 €/kW h. The two cases could contribute 5.6% and 9.6% of the total energy requirement for full utilisation of the soy sauce plant. Combining the process integration and solar heat supply measures, steam supply from the steam plant could be reduced by up to 14%.

In future work, further techno-economic analysis will be conducted to compare the use of solar thermal, PV, and industrial heat pumps for the generation of all local demands on an industrial level (electricity, heating, and cooling). The goal of this will be to elucidate the lowest cost combination of environmentally friendly technologies to meet process demands.

Acknowledgements

The authors wish to acknowledge the Engineering and Physical Science Research Council (EPSRC) for funding of this work within the GLOBAL Sustainable Energy through China-UK Research Engagement (SECURE) programme (project number EP/K004689/1) and the European Union for funds received through the People Programme (Marie Curie Actions) of the Seventh Framework Programme FP7/2007-2013/under REA grant agreement no 317085 (PITN-GA-2012-317085), commonly known at the SHINE (Solar Heat Integration Network) Program (http://www.uni-kassel.de/maschinenbau/institute/ite/solnet-shine.html). The authors further wish to thank Mr. Wolfgang Striewe from Industrial Solar GmbH for his advice and provision of some calculations.

Data supporting this publication is not openly available due to commercial considerations. Additional metadata record at 10.17634/120693-1. Please contact Newcastle Research Data Service at rdm@ncl.ac.uk for further information.

References

[1] BP. BP statistical review of World Energy June 2012; 2012. <http://www.bp.com/assets/bp_internet/globalbp/globalbp_uk_english/reports_and_publications/statistical_energy_review_2011/STAGING/local_assets/pdf/statistical_review_of_world_energy_full_report_2012.pdf> [accessed 04.10.13].
[2] CSY. China statistical yearbook 2011. Beijing, PR China: China Statistic Press, National Bureau of Statistics 2011.
[3] Yu F, Han F, Cui ZJ. Reducing carbon emissions through industrial symbiosis: a case study of a large enterprise group in China. J Clean Prod 2015;103:811–8.
[4] Business insider. China energy use 2012; 2012. <http://www.businessinsider.com/china-energy-use-2012-8?op=1> [accessed 20.04.15].
[5] CCTV. The great divide of environmental protection: the loss due to pollution in China each year 10% of GDP; nd. <http://finance.cctv.com/20070319/100794.shtml> [accessed 10.04.15].
[6] Liu LQ, Wang ZX, Zhang HQ, Xue YC. Solar energy development in China – a review. Renew Sustain Energy Rev 2010;14(10):301–11.
[7] NBS. China statistical yearbook 2014. Beijing: National Bureau of Statistics, China Statistics Press; 2014.
[8] NBS. China statistical yearbook 2011. Beijing: National Bureau of Statistics, China Statistics Press; 2011.
[9] Feng YY, Chen SQ, Zhang LX. System dynamics modeling for urban energy consumption and CO_2 emissions: a case study of Beijing, China. Ecol Model 2013:44–52.
[10] Li Z, Tong LZ, Sun J. Analysis of energy consumption in Beijing. China's Foreign Trade 2010;1:58–61.
[11] Shen B, Price L, Lu H. Energy audit practice in China: national and local experiences and issues. Energy Policy 2012;46:346–58.
[12] Qi Y, Wu T, He J, King DA. China's carbon conundrum. Nat Geosci 2013;6:507–9.
[13] World Bank. Accelerating energy conversion in China's Provinces. Washington, DC: World Bank; 2010. <http://documents.worldbank.org/curated/en/2010/06/12720925/accelerating-energy-conservation-chinas-provinces> [accessed 14.09.15].
[14] Zhao XF, Li HM, Wu LA, Qi Y. Implementation of energy-saving policies in China: how local governments assisted industrial enterprises in achieving energy-saving targets. Energy Policy 2014;66:170–84.
[15] Bai YY, Jie Y, Guo YJ, Song D. An innovative system for promoting cleaner production: mandatory cleaner production audits in China. J Clean Prod; 2015. http://dx.doi.org/10.1016/j.clepro.2015.07.107 [in press].
[16] Thollander P, Paramonova S, Cornelis E, Kimura O, Trianni A, Karlsson M, et al. International study on energy end-use data among industrial SMEs (small and medium-sized enterprises) and energy end-use efficiency improvement opportunities. J Clean Prod 2015;104:282–96.
[17] Trianni A, Cagno E, Farne S. Barriers. Drivers and decision-making process for industrial energy efficiency: abroad study among manufacturing small and medium-sized enterprises. Appl Energy; 2015. http://dx.doi.org/10.1016/j.apenergy.2015.02.078 [in press].
[18] Kannan R, Boie W. Energy management practice in SME – case study of a German Bakery. Energy Convers Manage 2003;44:945–59.
[19] Sturm B, Hugenschmidt S, Joyce S, Hofacker W, Roskilly AP. Opportunities and barriers for efficient energy use in a medium sized brewery. Appl Therm Eng 2013;53(2):397–404.
[20] AlQdah K. Potential opportunities for energy saving in a Jordanian poultry company. Energy Convers Manage 2010;51:1651–5.
[21] Priambodo A, Kumar S. Energy use and carbon dioxide emission of Indonesian small and medium scale industries. Energy Convers Manage 2001;42:1335–48.
[22] Schnitzer H, Brunner C, Gwehenberger G. Minimizing greenhouse gas emissions through the application of solar thermal energy in industrial processes. J Clean Prod 2006;15(13–14):1271–86.
[23] Mekahilefa S, Saidur R, Safari A. A review on solar energy use in industry. Renew Sustain Energy Rev 2011;15(4):1777–90.
[24] IEA. Technology roadmap solar heating and cooling; nd. <https://www.iea.org/publications/freepublications/publication/technology-roadmap-solar-heating-and-cooling.html> [accessed 23.04.15].
[25] IEA. Technology roadmap solar PV energy; 2014. <http://www.iea.org/media/freepublications/technologyroadmaps/solar/TechnologyRoadmapSolarPhotovoltaicEnergy_2014edition.pdf> [accessed 20.06.15].
[26] Muster-Slawitsch B, Weiss W, Schnitzer H, Brunner C. The green brewery concept – energy efficiency and the use of renewable energy sources in breweries. Appl Therm Eng 2011;31(13):2123–34.
[27] Schmitt B. Integration thermischer Solaranlagen zur Bereitstellung von Prozesswärme in Industriebetrieben. Schriftenreihe der Reiner Lemoine-Stiftung: Shaker Verlag, Aachen; 2014.
[28] Muster B, Schmitt B, Krummenacher P, Helmke A, Ben Hassaine I. IEA: IEA SHC TASK 49/IV Integration Guideline; 2014. <http://task49.iea-shc.org/data/sites/1/publications/150218_IEA%20Task%2049_D_B2_Integration_Guideline-final.pdf> [accessed 03.05.15].
[29] Weinstock D, Appelbaum J. Optimal solar field design of stationary collectors. Trans ASME 2004;126:898–905.
[30] Weinstock D, Appelbaum J. Optimization of economic solar field design of stationary solar collectors. J Solar Energy Eng 2007;129:363–70.
[31] Kikkoman. Future vision of Kikkoman group. Global vision 2020; 2009. <http://www.kikkoman.com/corporateprofile/globalvision/pdf/gv2020_e.pdf> [accessed 04.10.13].
[32] Luh BS. Industrial production of soy sauce. J Ind Microbiol 1995;14:467–71.
[33] Beuchat LR. Food and beverage mycology. 2nd ed. USA: AVI; 1987.
[34] Lewis. Physical properties of food and food processing systems. Cambridge, UK: Woodhead Publishing Series in Food Science, Technology and Nutrition No. 23, Woodhead; 1996.
[35] Rahman MS. Food properties handbook. Bocca Rota, Florida, USA: CRC Press; 2009.
[36] Stahl; 2013. <http://www.sachverstand-gutachten.de/wissenswertes/MB_821.pdf> [accessed 12.03.13].
[37] Rudolf W. Industrial wastes, their disposal and treatment. New York: Reinhold Publishing Corp; 1953.
[38] Reay D. The role of process intensificatnoin in cutting greenhouse gas emissions. Appl Therm Eng 2008;28:2011–9.

[39] Duffie JA, Beckman WA. Solar engineering of thermal processes. 3rd ed. John Wiley & Sons; 2006.
[40] Despotovic M, Nedic V. Comparison of optimum tilt angles of solar collectors determined at yearly, seasonal and monthly levels. Energy Convers Manage 2015;97:121–31.
[41] Al-Salaymeh A, Al-Rawabdeh I, Emran S. Economical investigation of an integrated boiler–solar energy saving system in Jordan. Energy Convers Manage 2010;51(8):1621–8.
[42] Mokheimer EM, Dabwan YN, Habib MA, Said SA, Al-Sulaiman FA. Techno-economic performance analysis of parabolic trough collector in Dhahran, Saudi Arabia. Energy Convers Manage 2014;86:622–33.
[43] Sun J, Liu Q, Hong H. Numerical study of parabolic-trough direct steam generation loop in recirculation mode: characteristics, performance and general operation strategy. Energy Convers Manage 2015;96:287–302.
[44] Lauterbach C. Potential, system analysis and preliminary design of a low temperature solar process heat systems. Kassel University Press; 2014.
[45] VDI. VDI 6002 Blatt 1 + 2 Solare Trinkwassererwärmung, VDI Verlag; 2014.
[46] CPI. Historic inflation China. CPI China; 2014. <http://www.inflation.eu/inflation-rates/china/historic-inflation/cpi-inflation-china.aspx> [accessed 16.03.14].
[47] Chinese Government. Steam prices Beijing; 2014. <http://govinfo.nlc.gov.cn/bjfz/xxgk/bjskfqgwh/201107/t20110725_935172.html?classid=355> [accesses 20.02.14].
[48] Shanghai Jiao Tong University, private communication.
[49] Shah V, Booream-Phelps J. Crossing the chasm: solar grid parity in a low oil price era; 2015.
[50] Kalogirou S. Thermal performance, economic and environmental life cycle analysis of thermosiphon solar water heaters. Solar Energy 2009;83(1):39–48.
[51] Branker K, Pathak MJM, Pearce JM. A review of solar photovoltaic levelized cost of electricity. Renew Sustain Energy Rev 2011;15(9):4470–82.
[52] Hess S, Oliva A. Solar process heat generation: guide to solar thermal design for selected industrial processes. Germany: Freiburg; 2011.